Journal of Power Sources 195 (2010) 8071–8074

Contents lists available at ScienceDirect

Journal of Power Sources

journal homepage: www.elsevier.com/locate/jpowsour

Short communication

$Sr_2Fe_{4/3}Mo_{2/3}O_6$ as anodes for solid oxide fuel cells

Guoliang Xiao, Qiang Liu, Xihui Dong, Kevin Huang, Fanglin Chen*

Department of Mechanical Engineering, University of South Carolina, Columbia, SC 29208, United States

ARTICLE INFO

Article history:
Received 2 June 2010
Received in revised form 10 July 2010
Accepted 12 July 2010
Available online 17 July 2010

Keywords:
Solid oxide fuel cells
Anode
Perovskite
Electrochemical performance

ABSTRACT

$Sr_2Fe_{4/3}Mo_{2/3}O_6$ has been synthesized by a combustion method in air. It shows a single cubic perovskite structure after being reduced in wet H_2 at 800 °C and demonstrates a metallic conducting behavior in reducing atmospheres at mediate temperatures. Its conductivity value at 800 °C in wet H_2 (3% H_2O) is about 16 S cm^{-1}. This material exhibits remarkable electrochemical activity and stability in H_2. Without a ceria interlayer, maximum power density (P_{max}) of 547 mW cm^{-2} is achieved at 800 °C with wet H_2 (3% H_2O) as fuel and ambient air as oxidant in the single cell with the configuration of $Sr_2Fe_{4/3}Mo_{2/3}O_6$|$La_{0.8}Sr_{0.2}Ga_{0.83}Mg_{0.17}O_3$ (LSGM)| $La_{0.6}Sr_{0.4}Co_{0.2}Fe_{0.8}O_3$ (LSCF). The P_{max} even increases to 595 mW cm^{-2} when the cell is operated at a constant current load at 800 °C for additional 15 h. This anode material also shows carbon resistance and sulfur tolerance. The P_{max} is about 130 mW cm^{-2} in wet CH_4 (3% H_2O) and 472 mW cm^{-2} in H_2 with 100 ppm H_2S. The cell performance can be effectively recovered after changing the fuel gas back to H_2.

1. Introduction

As one of the cleanest and most efficient power generation devices, solid oxide fuel cell (SOFC) has drawn considerable attentions from worldwide researchers in the past few decades. In particular, the high operating temperature makes SOFC directly utilize hydrocarbon fuels possible [1–5]. This feature makes the system design much simplified and reduces the cost. However, the state-of-the-art Ni-containing anodes presently used in SOFC are susceptible to carbon formation and sulfur poisoning, both of which would severely deteriorate the cell performance, making the direct oxidation of sulfur-containing hydrocarbon fuels impossible [6,7]. Therefore, there is a growing need in developing a new class of anode materials with carbon resistance and sulfur tolerance for the low-cost, direct hydrocarbon fueled SOFCs.

Ceramic oxides have emerged as the potential candidates for the direct oxidation anodes in the past few years, among which perovskite oxides have received the most attention due to the exhibited high mixed conductivity and good electrochemical activity in reducing atmospheres [8]. For instance, $(La_{1-x}Sr_x)_{0.9}Cr_{0.5}Mn_{0.5}O_3$ was reported to show reasonably good performance at 900 °C in wet CH_4 (3% H_2O) without carbon formation when used as an anode material in SOFCs [9–11]. $La_4Sr_8Ti_{11}Mn_{0.5}Ga_{0.5}O_{37.5}$ is another example of potential anode exhibiting good catalytic activity to wet H_2 and CH_4 at 950 °C [12]. At lower SOFC operating temperatures, however, the catalytic activity of these materials is insufficient. Recently, Huang and Goodenough have demonstrated a new class of anode materials Sr_2MMoO_6 (M = Mn, Ni, Co) with double perovskite structure [13,14]. The SOFCs using such anode compositions have showed good electro-catalytic activities and sulfur tolerance. When combined with ceria based interlayer and Pt current collector, impressive performance was obtained at intermediate temperatures. Sr_2NiMoO_6 was also reported to have excellent performance with H_2 in absence of ceria interlayer and Pt current collector [15]. These results suggest that the double perovskite type oxides have resistance to carbon formation and tolerance to sulfur, and therefore have a great potential to be anode materials for direct hydrocarbon fueled SOFCs.

In addition to the double perovskite type anode materials mentioned above, Sr_2FeMoO_6 is another interesting candidate. It has been investigated as a ferromagnetic material and is stable in reducing atmospheres due to the protection of the Mo^{4+}/Mo^{5+} redox couple that prevents Fe^{3+} from being reduced to Fe^{2+} [16,17]. Since in air the most preferable oxidation state of Mo is +6, the phase of Sr_2FeMoO_6 would not form in air. Special cares are needed during SOFC fabrication in order to ensure the formation of the desirable phase. Although Sr_2FeMoO_6 has recently been reported as an anode in SOFCs by firing the anode in a protective atmosphere [18], it is still needed to explore $Sr_2Fe_{1+x}Mo_{1-x}O_6$ with different Fe and Mo ratios, so that it can be synthesized in air, or at least it can be formed under the fuel cell operating condition.

In this paper, $Sr_2Fe_{1+x}Mo_{1-x}O_6$ (x = 0, 0.15, 1/3) have been synthesized by a combustion method. The $Sr_2Fe_{4/3}Mo_{2/3}O_6$ composition can be easily reduced at 800 °C to form a single phase double perovskite. The performance of

* Corresponding author. Tel.: +1 803 777 4875; fax: +1 803 777 0106.
E-mail address: chenfa@cec.sc.edu (F. Chen).

0378-7753/$ – see front matter © 2010 Elsevier B.V. All rights reserved.
doi:10.1016/j.jpowsour.2010.07.036

the single cell $Sr_2Fe_{4/3}Mo_{2/3}O_6$|$La_{0.8}Sr_{0.2}Ga_{0.83}Mg_{0.17}O_3$ (LSGM)|$La_{0.6}Sr_{0.4}Co_{0.2}Fe_{0.8}O_3$ (LSCF) has been evaluated by using H_2, CH_4, or sulfur-containing H_2 as fuel.

2. Experimental

2.1. Synthesis

$Sr_2Fe_{1+x}Mo_{1-x}O_6$ (x = 0, 0.15, 1/3) were synthesized by a glycine–nitrate combustion process (GNP). In a typical process, strontium nitrate (99%, Alfa Aesar), iron nitrate (99%, Alfa Aesar) and ammonium molybdate (99%, Mallinckrodt Baker) were dissolved in de-ionized water according to the stoichiometry. Citric acid was used to adjust the pH value of the solution and to prevent any precipitation, while glycine was used as a fuel for combustion. After being stirred for several hours, the solution was heated in a microwave oven until self-ignition. The combustion product, ash, was collected and subsequently calcined at 600 °C for 2 h and at 1100 °C for 5 h to remove any organic residues. The powders were then reduced in a flowing wet H_2 (3% H_2O) at 800 °C for 5 h for phase and structure analysis.

The $La_{0.8}Sr_{0.2}Ga_{0.83}Mg_{0.17}O_3$ (LSGM) electrolyte and $La_{0.6}Sr_{0.4}Co_{0.2}Fe_{0.8}O_3$ (LSCF) cathode powders were also prepared by the GNP method which was described elsewhere [19,20].

2.2. Characterizations

The powder X-ray diffraction (XRD) patterns were recorded on a D/MAX-3C X-ray diffractometer with graphite–monochromatized Cu-Kα radiation (λ=1.5418 Å) at a scanning rate of 5 min^{-1} in the 2θ range of 10–90°. MDI-Jade program was used to identify the phases and to analyze crystal structures of the samples. The microstructural morphology was characterized by scanning electron microscopy (SEM, FEI Quanta and XL 30).

The total electrical conductivity of $Sr_2Fe_{4/3}Mo_{2/3}O_6$ in a rectangular bar shape was measured in wet H_2 (3% H_2O) using the standard four terminal DC method. The pressed green bar was first sintered at 1400 °C for 5 h and then reduced at 800 °C in wet H_2 (3% H_2O) for 10 h before the conductivity measurement.

2.3. Single cell test

The single cell was fabricated on the LSGM electrolyte substrate made by pressing LSGM pellets and then sintering at 1400 °C for 5 h. The thickness of the LSGM pellets was about 300 μm. The inks of the $Sr_2Fe_{4/3}Mo_{2/3}O_6$ anode and the LSCF cathode were then screen printed on the two sides of the LSGM electrolyte pellet. The anode and the cathode together with the LSGM electrolyte were then co-fired in air at 1100 °C for 2 h. The thickness of the electrodes was about 20–30 μm. Au paste was printed on the anode surface while Pt paste was printed on the cathode surface as the contact layers for current collection. Au is inert to the fuel oxidation. Ambient air was used as oxidant. The flow rate of the fuel gases was set at 40 ml min^{-1}. The $Sr_2Fe_{4/3}Mo_{2/3}O_6$ anode was reduced in situ upon exposure to wet H_2 (3% H_2O) at 800 °C for 5 h. Before any electrochemical measurement, the cell was stabilized at least for 1 h each time when the fuel gas was switched.

3. Results and discussion

3.1. Phase, structure and conductivity

Fig. 1 shows the XRD patterns of $Sr_2Fe_{1+x}Mo_{1-x}O_6$ (x = 0, 0.15, 1/3) before and after reduction at 800 °C in wet H_2 (3% H_2O). It is evident that the oxidized samples (calcined at 1100 °C for 5 h in air) contain multiple phases. The major impurity can be indexed as $SrMoO_4$ (JCPDS 08-0482). The impurity peaks become weaker with the decrease of the Mo concentration in the compound. Upon reduction at 800 °C in H_2, $Sr_2Fe_{4/3}Mo_{2/3}O_6$ shows a cubic perovskite structure with no impurity peak detectable in the XRD pattern. The calculated lattice parameter of $Sr_2Fe_{4/3}Mo_{2/3}O_6$ is 7.878(3) Å, which is consistent with the reported value [21].

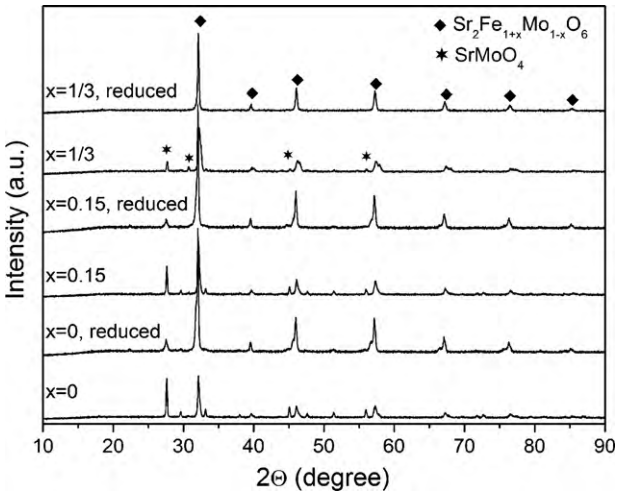

Fig. 1. XRD patterns of $Sr_2Fe_{1+x}Mo_{1-x}O_6$ (x = 0, 0.15, 1/3) synthesized in air and reduced at 800 °C in wet H_2 (3% H_2O).

The conductivity of $Sr_2Fe_{4/3}Mo_{2/3}O_6$ as a function of temperature is shown in Fig. 2. In the temperature range 370–830 °C studied, the electrical conduction follows the metallic behavior that the value decreased while the temperature increased. At 800 °C, it was about 16 S cm^{-1}.

3.2. Single cell performance

The LSGM electrolyte supported fuel cell with $Sr_2Fe_{4/3}Mo_{2/3}O_6$ as the anode was tested with wet H_2 (3% H_2O) as the fuel and air as the oxidant. Before testing, the cell was held at 800 °C for 5 h in order to reduce the anode. Fig. 3 shows the cell voltage and power density as a function of current density at different temperatures. The maximum power density (P_{Max}) of the cell reached 268, 392, 547 mW cm^{-2} at 700, 750 and 800 °C, respectively.

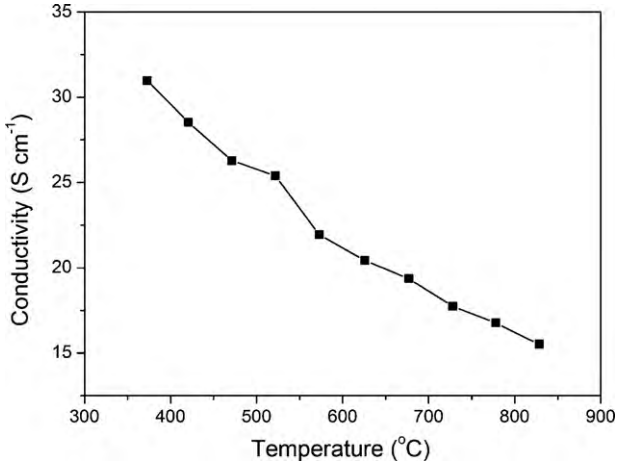

Fig. 2. Conductivity measured in wet H_2 (3% H_2O) on the $Sr_2Fe_{4/3}Mo_{2/3}O_6$ bar sintered in air at 1400 °C. The bar was reduced at 800 °C in the testing atmosphere for 10 h before test.

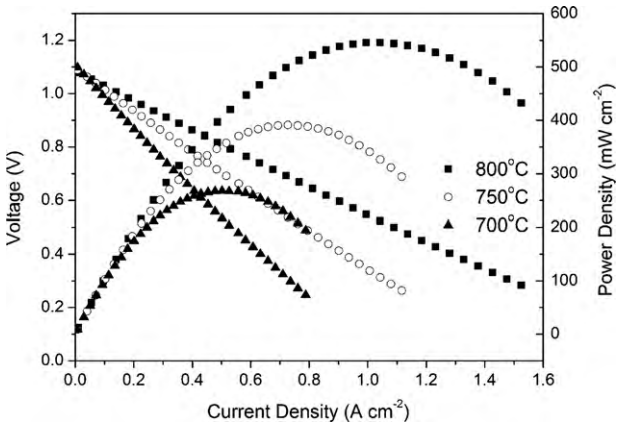

Fig. 3. Cell voltage and power density as a function of current density in wet H_2 (3% H_2O) of the single cell with $Sr_2Fe_{4/3}Mo_{2/3}O_6$ anode, LSGM electrolyte and LSCF cathode at 700, 750 and 800 °C.

The electrochemical impedance spectra at different temperatures were also measured under open-circuit conditions and the results are shown in Fig. 4a. The high frequency intercept on the real axis represents the total ohmic resistance of the cell (R_{ohm}). The low frequency intercept on the real axis represents the total cell resistance (R_{total}). The difference between the two is the electrode polarization resistance (R_p), including the contribution from both the cathode and anode. The values of R_p, R_{ohm} and R_{total} of the cell at 700, 750 and 800 °C are plotted in Fig. 4b. It can be seen that the total resistance was mainly dominated by R_{ohm}. The value of R_{ohm} at 800 °C was about 0.4 Ω cm^2. It is higher than that reported with a 300-μm thick LSGM electrolyte supported cell using a Sr_2FeMoO_6 anode due to the lower electrical conductivity of $Sr_2Fe_{4/3}Mo_{2/3}O_6$ compared with that of Sr_2FeMoO_6, which is about 200 S cm^{-1} at 800 °C in H_2 [18]. However, the $R_p \sim 0.2$ Ω cm^2 at 800 °C is lower than that of Sr_2FeMoO_6, which is about 0.3 Ω cm^2 at 800 °C [18].

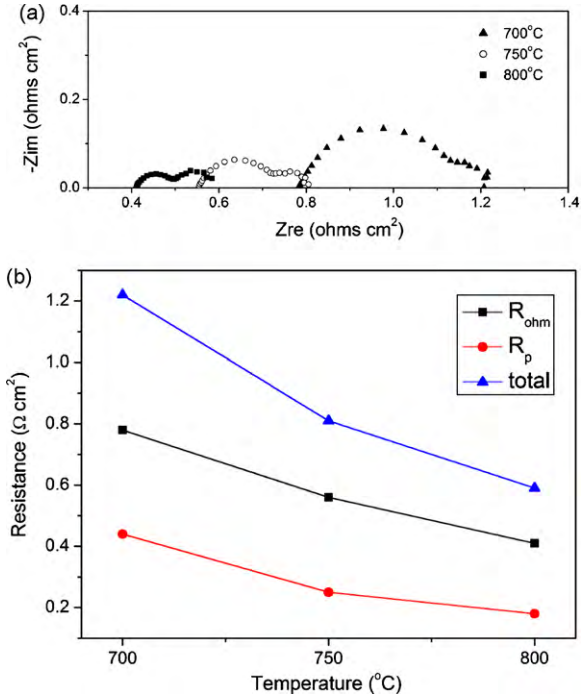

Fig. 4. Impedance spectra and resistances of a single cell measured at 700, 750 and 800 °C under open-circuit conduction: (a) impedance spectra of the single cell at different temperature and (b) the ohmic resistance (R_{ohm}), the polarization resistance (R_p) and the total resistance (R_{total}) of the single fuel cell.

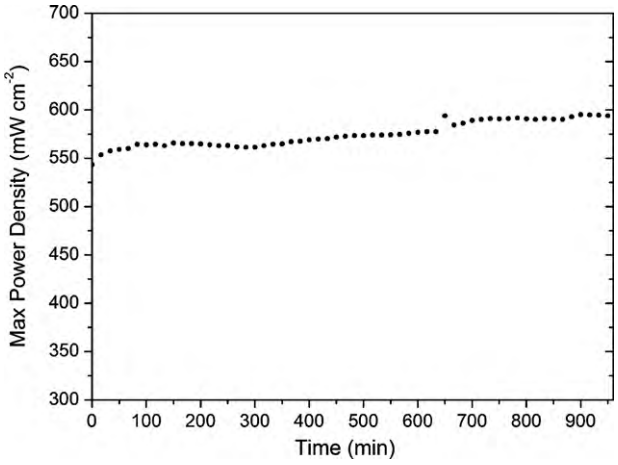

Fig. 5. Electrochemcial stability of a single cell with $Sr_2Fe_{4/3}Mo_{2/3}O_6$ anode at 800 °C in wet H_2 (3% H_2O).

The lower R_p is probably due to the increased concentration of oxygen vacancies by increasing the Fe/Mo ratio in $Sr_2Fe_{4/3}Mo_{2/3}O_6$, resulting in a higher catalytic activity [22].

3.3. Stability, carbon resistance and sulfur tolerance

The stability of the $Sr_2Fe_{4/3}Mo_{2/3}O_6$ anode was investigated by operating the single cell at P_{max} (the current density was set at 1020 mA cm^{-2} according to the voltage–current density curve) in wet H_2 for 16 h at 800 °C. As shown in Fig. 5, a slight improvement in the cell performance was observed and the P_{max} reached 595 mW cm^{-2} at 800 °C at the end of the tested period. This result demonstrates that $Sr_2Fe_{4/3}Mo_{2/3}O_6$ is a very promising anode material with very good performance stability under the fuel cell operating conditions. It further indicates that there exists no compatibility issues between the $Sr_2Fe_{4/3}Mo_{2/3}O_6$ anode and LSGM electrolyte and a ceria interlayer is not needed.

The electrochemical performance of the $Sr_2Fe_{4/3}Mo_{2/3}O_6$ anode for direct utilization of hydrocarbon fuel and for sulfur tolerance was also investigated by testing the cell in wet CH_4 (3% H_2O) and H_2 containing 100 ppm H_2S. As shown in Fig. 6, the maximum power density, P_{max} reached 130 mW cm^{-2} in wet CH_4 at 800 °C. Further, post-test analysis showed no carbon deposition on the $Sr_2Fe_{4/3}Mo_{2/3}O_6$ anode, indicating that $Sr_2Fe_{4/3}Mo_{2/3}O_6$ is a promising anode for direct hydrocarbon utilization. On the other hand, the maximum power density, P_{max} was 472 mW cm^{-2} when the fuel was switched from wet H_2 to H_2 containing 100 ppm H_2S,

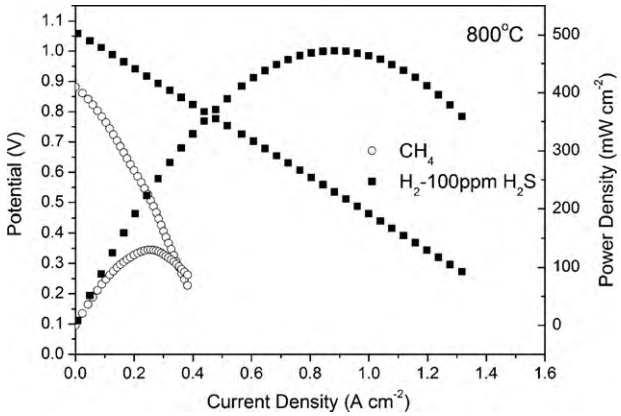

Fig. 6. Cell voltage and power density as a function of current density in wet CH_4 (3% H_2O) and H_2 with 100 ppm H_2S at 800 °C.

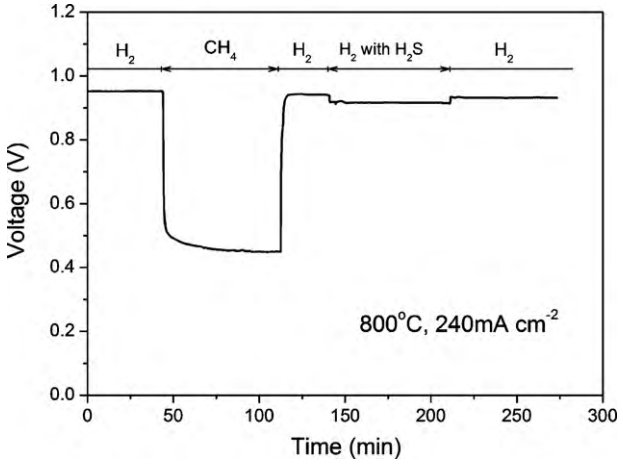

Fig. 7. Voltage change of the single cell in different fuel gas at 800 °C at 240 mA cm^{-2} current density when switching the fuel gas between wet H_2 (3% H_2O), wet CH_4 (3% H_2O) and H_2 with 100 ppm H_2S.

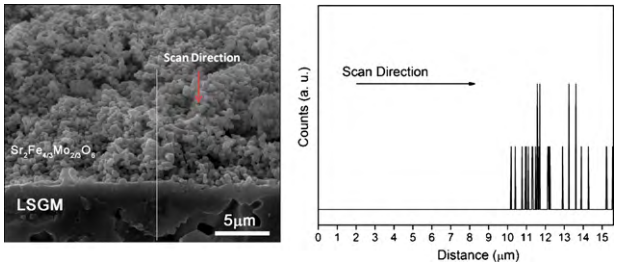

Fig. 8. EDX line scan of La. La signal was not found in the anode after the test.

showing very little cell performance drop in sulfur-containing fuels.

In order to investigate the performance stability of fuel cells with the $Sr_2Fe_{4/3}Mo_{2/3}O_6$ anode in different fuels, a constant current density of 240 mA cm^{-2} was applied to the cell at 800 °C and the cell voltage was monitored while the cell was exposed to different fuels. As shown in Fig. 7, a sharp decrease in cell voltage from 0.96 V to around 0.5 V was observed after the fuel was switched from wet H_2 to wet CH_4 (3% H_2O) due to the low catalytic activity of $Sr_2Fe_{4/3}Mo_{2/3}O_6$ anode in CH_4 compared with that in H_2. The cell voltage gradually became stable and it was about 0.45 V after being operating for 1 h in CH_4. However, the cell voltage immediately recovered back to 0.94 V after the fuel gas was switched from CH_4 back to wet H_2. Similar behavior was also observed when the fuel gas was switched between wet H_2 and H_2 with 100 ppm H_2S. The cell voltage was 0.91 V in H_2 with 100 ppm H_2S and recovered to 0.93 V after the fuel gas was switched from H_2 with 100 ppm H_2S back to wet H_2 again. These results suggest that $Sr_2Fe_{4/3}Mo_{2/3}O_6$ is a very promising anode material to directly utilize hydrocarbon and sulfur contained fuels.

The EDX line scan result of the interface between the $Sr_2Fe_{4/3}Mo_{2/3}O_6$ anode and LSGM electrolyte after the cell performance testing is shown in Fig. 8. No La signal has been observed in the anode region, indicating that there are no compatibility issues when using the $Sr_2Fe_{4/3}Mo_{2/3}O_6$ anode and LSGM electrolyte without the ceria interlayer.

As it is reported on Sr_2MgMoO_6, the properties of these double perovskite oxides are strongly affected by the states of B-site cations, such as the ratio of the cations and the degree of the cation ordering [21,23]. By comparing the single cell performance of $Sr_2Fe_{1+x}Mo_{1-x}O_6$ anode with different Fe/Mo ratios reported recently [18,24], it can be found that both the Mo content and the intrinsic oxygen vacancies determined by the Fe/Mo ratio play important roles in the anode catalytic activity. However, further fundamental studies are needed in order to elucidate the mechanism of these influencing factors.

4. Conclusions

$Sr_2Fe_{4/3}Mo_{2/3}O_6$ has been synthesized in air by the glycine–nitrate combustion method. A pure perovskite phase was obtained by reducing the synthesized powder at 800 °C in wet H_2 (3% H_2O). The electrical conductivity of the reduced $Sr_2Fe_{4/3}Mo_{2/3}O_6$ shows a metallic behavior from 370 to 830 °C in wet H_2 (3% H_2O). The single cell performance evaluation using $Sr_2Fe_{4/3}Mo_{2/3}O_6$ as the anode indicates good catalytic activity and stability in H_2 and also shows the potential to utilize hydrocarbon and sulfur-containing fuels directly. Although long term stability test of $Sr_2Fe_{4/3}Mo_{2/3}O_6$ is still needed, this material shows the potential to be a promising candidate anode material for SOFCs.

Acknowledgements

We gratefully acknowledge the financial support of Heterogeneous Functional Materials for Energy Systems, an EFRC funded by DoE Office of Basic Energy Sciences under Award Number DE-SC0001061, the South Carolina Space Grant Consortium, the USC Future Fuels Initiative, the USC NanoCenter, and the USC Promising Investigator Research Award.

References

[1] K. Huang, J.B. Goodenough, Solid Oxide Fuel Cell Technology: Principles, Performance and Operations, Woodhead Publishing, Cambridge, 2009.
[2] A. Atkinson, S. Barnett, R.J. Gorte, J.T.S. Irvine, A.J. McEvoy, M.B. Mogensen, S. Singhal, J. Vohs, Nat. Mater. 3 (2004) 17–27.
[3] Z.L. Zhan, S.A. Barnett, Science 308 (2005) 844–847.
[4] W. Zhu, C.R. Xia, J. Fan, R.R. Peng, G.Y. Meng, J. Power Sources 160 (2006) 897–902.
[5] D. Ding, Z.B. Liu, L. Li, C.R. Xia, Electrochem. Commun. 10 (2008) 1295–1298.
[6] Y. Matsuzaki, I. Yasuta, Solid State Ionics 132 (2000) 261–269.
[7] B.C.H. Steele, I. Kelly, H. Middleton, R. Rudkin, Solid State Ionics 28 (1988) 1547–1552.
[8] J.B. Goodenough, Y.H. Huang, J. Power Sources 173 (2007) 1–10.
[9] S.W. Tao, J.T.S. Irvine, J. Electrochem. Soc. 151 (2004) A252–A259.
[10] S.W. Tao, J.T.S. Irvine, Nat. Mater. 2 (2003) 320–323.
[11] S.W. Tao, J.T.S. Irvine, J.A. Kilner, Adv. Mater. 17 (2005) 1734–1737.
[12] J.C. Ruiz-Morales, J. Canales-Vías quez, C. Savaniu, D. Marrero-Lïopez, W. Zhou, J.T.S. Irvine, Nature 439 (2006) 568–571.
[13] Y.H. Huang, R.I. Dass, Z.L. Xing, J.B. Goodenough, Science 312 (2006) 254–257.
[14] Y.H. Huang, G. Liang, M. Croft, M. Lehtimaki, M. Karppinen, J.B. Goodenough, Chem. Mater. 21 (2009) 2319–2326.
[15] T. Wei, Y. Ji, X.W. Meng, Y.L. Zhang, Electrochem. Commun. 10 (2008) 1369–1372.
[16] J. Lindïen, T. Yamamoto, M. Karppinen, H. Yamauchi, T. Pietari, Appl. Phys. Lett. 76 (2000) 2925–2927.
[17] Cz. Kapusta, P.C. Riedi, D. Zajac, M. Sikora, J.M. De Teresa, L. Morellon, M.R. Ibarra, J. Magn. Magn. Mater. 242–245 (2002) 701–703.
[18] L. Zhang, Q. Zhou, Q. He, T. He, J. Power Sources 195 (2010) 6356–6366.
[19] L.G. Cong, T.M. He, Y.A. Ji, P.F. Guan, Y.L. Huang, W.H. Su, J. Alloys Compd. 348 (2003) 325–331.
[20] Y. Ji, J. Liu, T.M. He, L.G. Cong, J.X. Wang, W.H. Su, J. Alloys Compd. 353 (2003) 257–262.
[21] G.Y. Liu, G.H. Rao, X.M. Feng, H.F. Yang, Z.W. Ouyang, W.F. Liu, J.K. Liang, J. Alloys Compd. 353 (2003) 42–47.
[22] H. Falcón, J.A. Barbero, G. Araujo, M.T. Casais, M.J. Martínez-Lope, J.A. Alonso, J.L.G. Fierro, Appl. Catal. B: Environ. 53 (2004) 37–45.
[23] Y. Ji, Y.H. Huang, J.R. Ying, J.B. Goodenough, Electrochem. Commun. 9 (2007) 1881–1885.
[24] Q. Liu, X.H. Dong, G.L. Xiao, F. Zhao, F.L. Chen, Adv. Mater. (2010), doi:10.1002/adma201001044, in press.